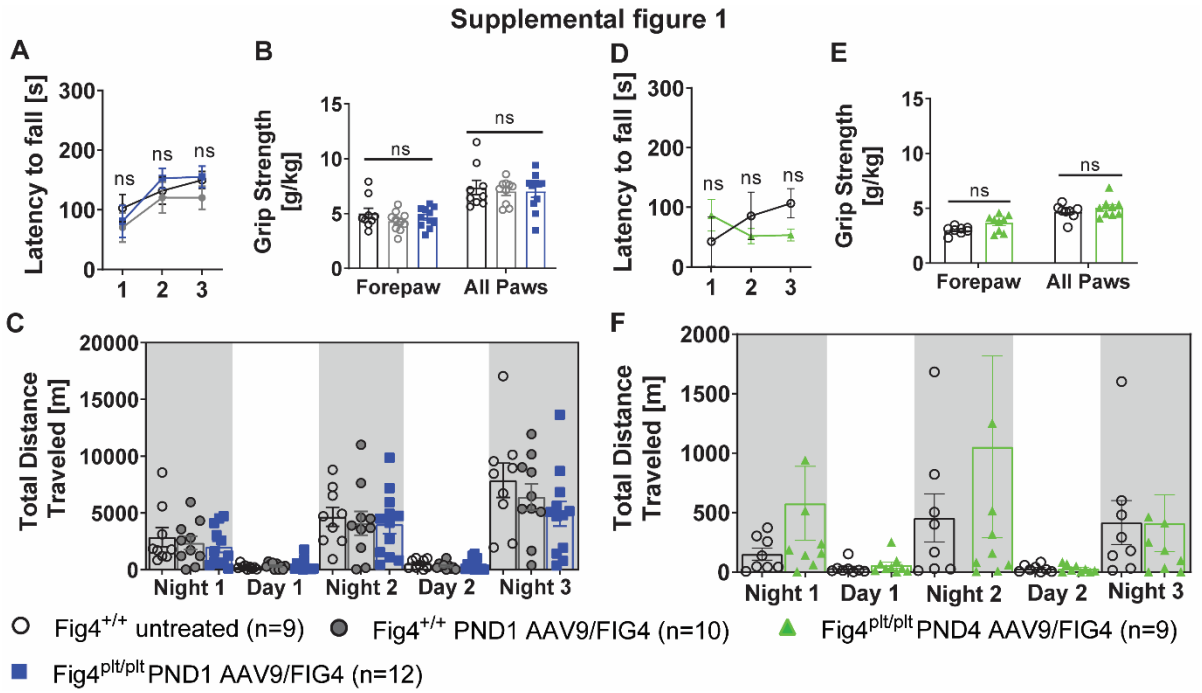

Supplemental figure 1: Neonatal treatment of *Fig4*$^{plt/plt}$ mice with AAV9/*FIG4* improves behavioral outcomes.
Fig4$^{plt/plt}$ mice treated at PND1 or 4 by ICV injection of the maximum AAV9/FIG4 dose were analyzed at 6 months-of-age for motor coordination performance, grip strength and general activity, N=12 for PND1 and N=9 for PND4 treatments. (A and D) Rotarod analysis is reported as the latency to fall during three trials. (B and E) Average grip strength normalized to body weight in the fore paws and all paws is shown. (C and F) General activity was assessed by monitoring voluntary wheel running, the average total distance traveled at each day time cycle is reported. All data represents the average ±SEM of combined males and females, since no significant differences were observed by sex. Groups were compared by two-way ANOVA with Dunnett test correction for multiple comparisons, ns = not significant.

Supplemental Table 1: Histopathology analysis of Fig4 wild type mice untreated or injected ICV with AAV9/FIG4 at six months post-treatment.

	Six months post-treatment	
Tissue	***Fig4*$^{+/+}$ untreated***	***Fig4*$^{+/+}$ PND1 AAV9-FIG4****
Brain	Normal	No well-defined cytoplasmic vacuoles that displace or compress a nucleus are found in any cell.
Spinal Cord-Cervical	Normal	No well-defined cytoplasmic vacuoles that displace or compress a nucleus are found in any cell.
Spinal Cord-Thoracic	Normal	No well-defined cytoplasmic vacuoles that displace or compress a nucleus are found in any cell.
Spinal Cord-Lumbar	One slide contains cells with 2 clear cytoplasmic vacuoles. Considered incidental finding.	One slide contains an oligodendrocyte with a moderate size vacuole compressing the nucleus. Considered incidental finding.
Dorsal root ganglion	Normal	No well-defined cytoplasmic vacuoles that displace or compress a nucleus are found in any cell.
Liver	Hepatocytes contain variable amounts of vacuolar change (glycogen), microvesicular and macrovesicular lipidosis, extramedullary hematopoiesis, and stromal lymphoplasmacytic infiltrate	Hepatocytes contain variable amounts of vacuolar change (glycogen), microvesicular and macrovesicular lipidosis, extramedullary hematopoiesis, and stromal lymphoplasmacytic infiltrate
Heart	Normal	Normal
Skeletal muscle	The tissues are normal	The tissues are normal
Kidney	Minimal to mild infiltrate of leukocytes considered as incidental findings.	Minimal to mild infiltrate of leukocytes considered as incidental findings.
Cervical lymph nodes	Lymph nodes are normal.	Lymph nodes are normal.
Mesenteric lymph nodes	Lymph nodes are normal.	Lymph nodes are normal.
Gonads	Testes and ovaries are normal.	Testes and ovaries are normal.

*N=6, 3 females/3 males. Necropsy at 6 months post-dosing.
** N=7, 4 females/3 males. Necropsy at 6 months post-dosing.

Half of the cohort treated at PND1, PND4 were euthanized at 6 months-of-age and brain, spinal cord, skeletal muscle, heart, liver, kidney, gonads, mesenteric and cervical lymph nodes were dissected. 10% NBF-fixed tissues were paraffin-embedded and 5 µm sections were stained with H&E. Histopathology analysis was conducted blinded for genotype and treatment by a board-certified veterinary pathologist at The Jackson Laboratory. The table summarize the major findings observed in *Fig4* wild type mice treated with AAV9-*FIG4* at 6 months post-injection.

Supplementary table 2: Frequency of HCC in control and AAV9/FIG4-treated mice.

Group	Treatment	Genotype	Age at Necropsy	Cohort size	# Mice with tumors	P-value vs Untreated
PND1	Untreated	WT	7-8 Months	11	0	
PND1	AAV9/FIG4	WT	7 Months	7	0	>0.9999
PND1 and PND4	AAV9/FIG4	HOM	7-8 Months	10	0	>0.9999
PND1	Untreated	WT	13 Months	9	2	
PND1	AAV9/FIG4	WT	13 Months	8	7	0.0152
PND1 and PND4*	AAV9/FIG4	HOM	11-13 Months	7	3	0.5962
*PND1: 1 HCC/4 mice. PND4: 2 HCC/3 mice.						

Supplemental table 2: Increased incidence of HCC in AAV9/*FIG4* treated mice
The table summarize the number of mice for each experimental group with hepatocellular carcinomas (HCC). Fisher's exact test was applied to determine statistical significance.

Supplemental figure 2

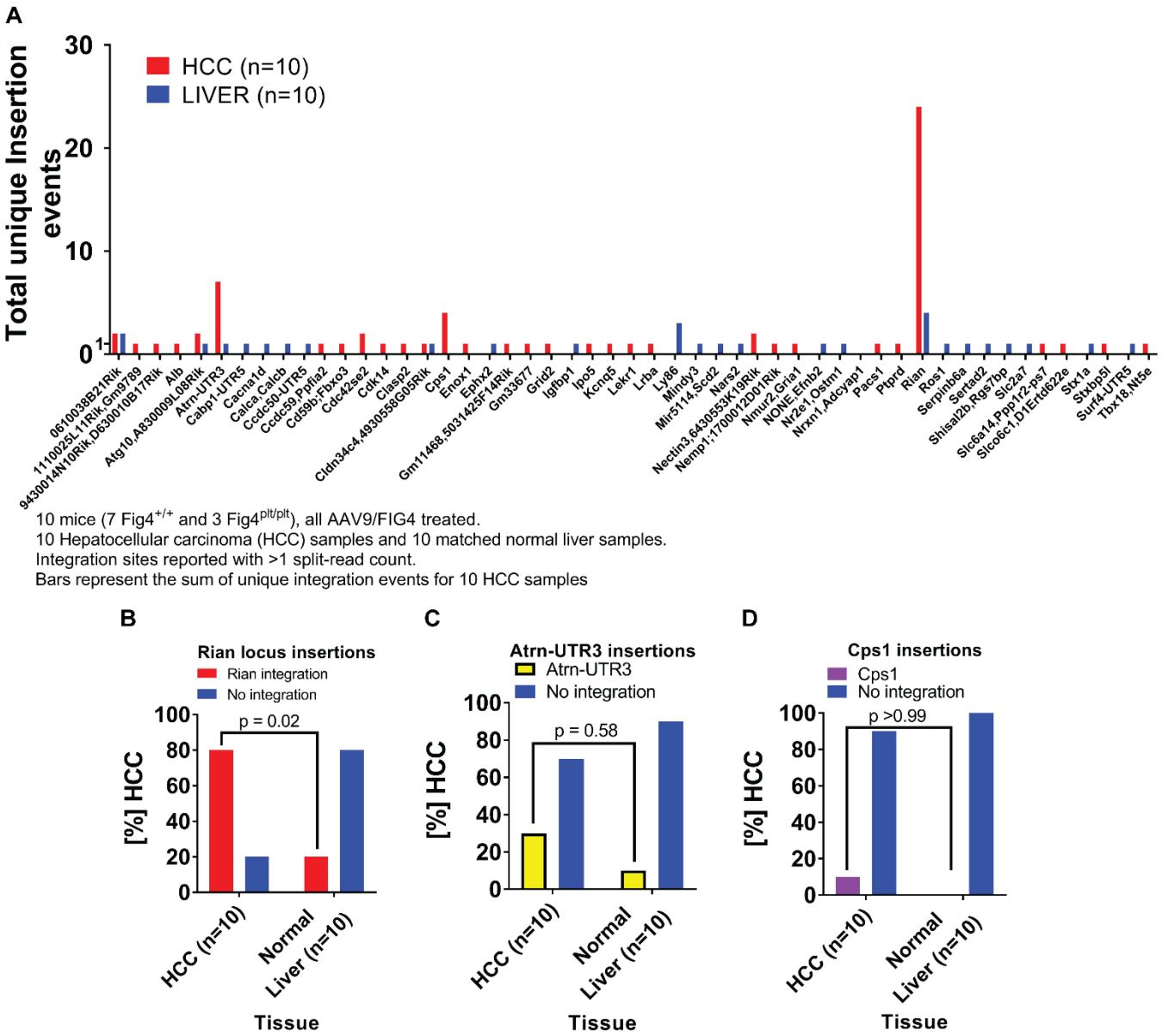

Supplemental figure 2: Whole genome sequence analysis of HCC shows significant integration events into *Rian* locus
One tumor mass was dissected from each mouse liver, together with a liver sample visually free of tumor. Sequencing libraries were generated and fed into Illumina sequencers (HiSeqX, Illumina). Two sequence analysis, two tools, Virus-Clip and BatVI were used to detect possible integration of viral vector. Split reads were identified and mapped to the mouse genome using both tools. (A) Represent the total number of unique insertion events at the genes/loci indicated on the *x* axes. Bottom panel indicates the incidence analysis for viral vector integration events into Rian locus (B), Atrn-UTR3 (C), Cps1 (D). Fisher's exact test was applied to determine statistical significance.

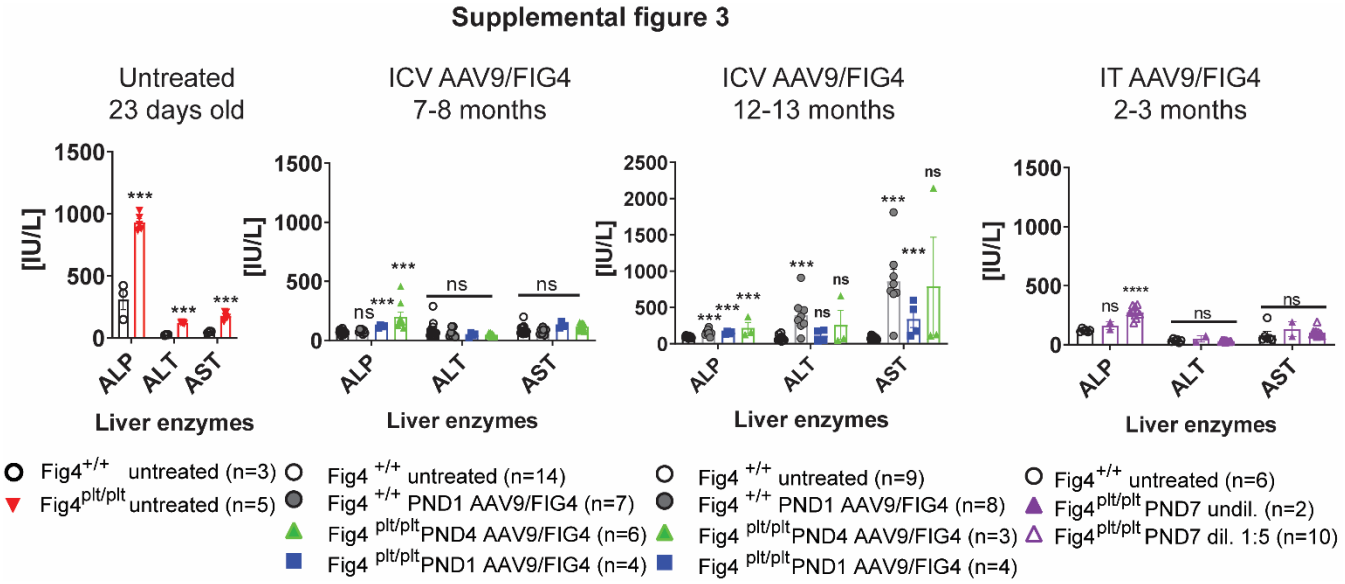

Supplemental figure 3: Liver enzymes levels in *Fig4*$^{plt/plt}$ mice.
Liver enzyme levels were assessed in serum from *Fig4*$^{plt/plt}$ and *Fig4*$^{+/+}$ mice either treated with AAV9/FIG4 or untreated. Number of mice and age are indicated in the figure. Statistical significance for comparisons between treatment groups and *Fig4*$^{+/+}$ untreated control, was determined using the Holm-Sidak method. ns = not significant, p>0.05, *** p<0.001, **** p<0.0001.

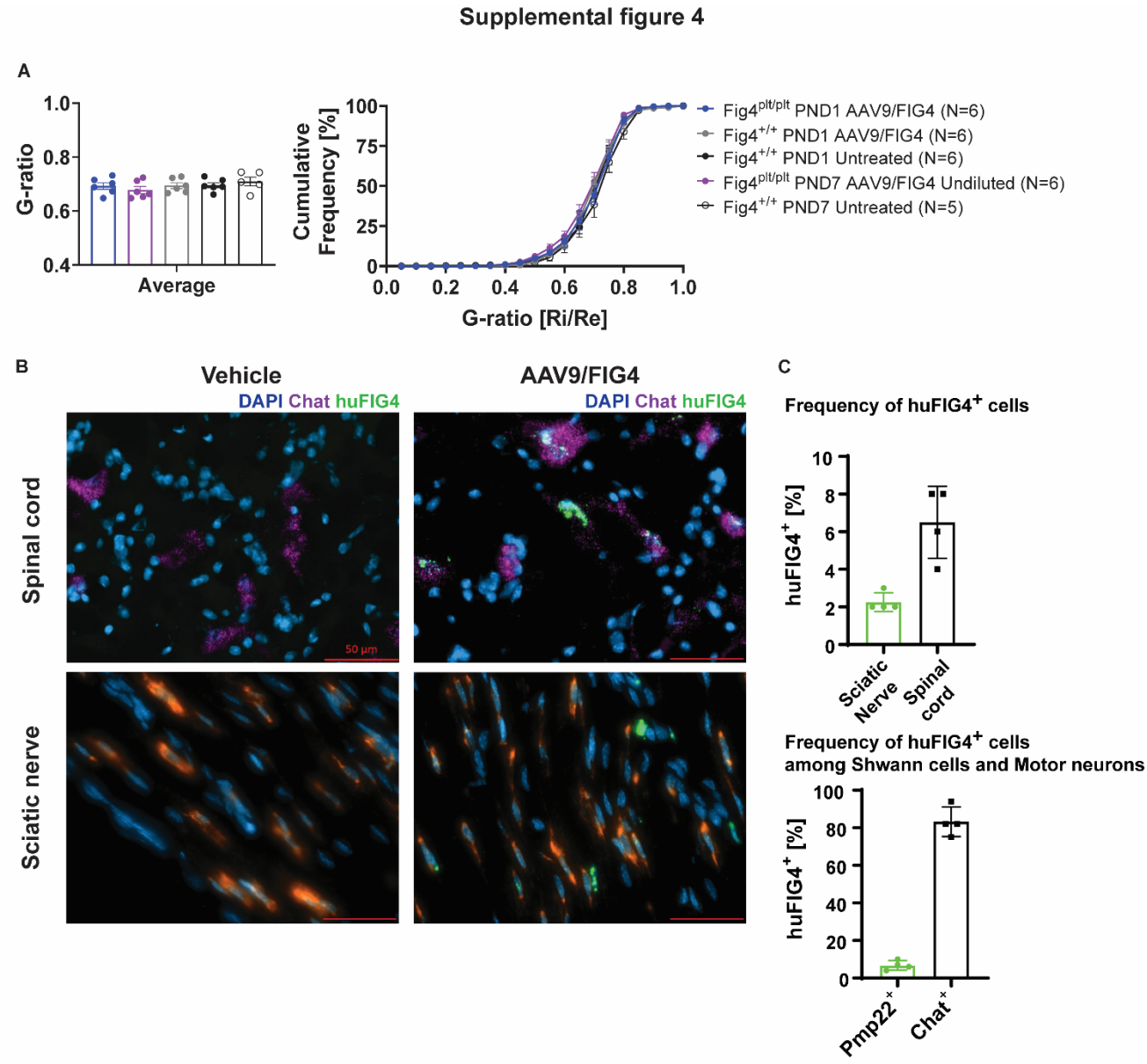

Supplemental figure 4: No demyelinating pathology after ICV and IT treatment with AAV9/FIG4. AAV9/FIG4 mRNA can be detected in motor neurons and Schwann cells after ICV injection.

Semi-thin sections of toluidine-blue stained sciatic nerve were analyzed for myelin thickness by measuring G-ratio. The internal and external area of a minimum of 100 axons by section was measured using ImageJ software. The area values were used to calculate the corresponding internal and external radius. G-ratio was calculated as the ratio between the internal radius (Ri) and the external radius (Re). (A) The average value for G-ratio on each treatment group is shown. The right panel shows the G-ratio distribution in a cumulative histogram, N=5 to 6 for each biological group. No differences were observed between biological groups (Two way ANOVA with Sidak's multiple comparisons test). (B) B6.C3H F1 mice matching the genetic background of *Fig4*^{plt} study mice were injected ICV at PND1 with AAV9/FIG4 ($5.4x10^{11}$ vg) or vehicle (n=4 per treatment group). Four weeks after injections, spinal cords and sciatic nerves were dissected and mounted in OCT freezing medium. Longitudinal 10 µm cryosections were processed, following vendor protocols, for mRNA detection by *in situ* hybridization, using RNAScope™ probes specific for *huFIG4*, *Pmp22* (Schwann cells) and *Chat* (motor neurons). (B) Representative images from spinal cord and sciatic nerve, showing double staining for *Chat/huFIG4* (spinal cord) and *Pmp22/huFIG4* (sciatic nerve). Scale bars represents 50 µm (C) Upper panel shows the percentage of cells expressing *huFIG4*, representing approximately 2% in sciatic nerve and 6% in spinal cord, with total cell number being assessed by DAPI-labeled nuclei. Lower panel indicates the frequency of *huFIG4* expressing cells among *Pmp22*-positive Schwann cells (7%) and *Chat*-positive motor neurons (80%). Bar graphs indicates the average ±SEM.